Joint Density-Functional Theory: Ab Initio Study of Cr_2O_3 Surface Chemistry in Solution

S. A. Petrosyan,*,† A. A. Rigos,‡ and T. A. Arias†

Department of Physics, Cornell University, Ithaca, New York 14853, and Department of Chemistry, Merrimack College, North Andover, Massachusetts 01845

Received: November 11, 2004; In Final Form: June 17, 2005

After introducing a new form of density-functional theory for the ab initio description of electronic systems in contact with a molecular liquid environment, we present the first detailed study of the impact of a solvent on the surface chemistry of Cr_2O_3, the passivating layer of stainless steel alloys. In comparison to a vacuum, we predict that the presence of water has little impact on the adsorption of chloride ions to the oxygen-terminated surface but has a dramatic effect on the binding of hydrogen to that surface. These results indicate that the dielectric screening properties of water are important to the passivating effects of the oxygen-terminated surface.

1. Introduction

Ab initio calculations have shed light on many physicochemical questions, including chemical reactions in solution and chemical reactions at surfaces.[1−3] Although computational chemistry is now able to provide not only qualitative but also quantitative insights into surface chemistry,[2] so far these studies have been limited to reactions in a vacuum, even though experimentally these reactions often occur in solvent environments. A fundamental roadblock to ab initio study of surface reactions in solution is that current continuum approaches do not sit on a firm theoretical foundation.

Each year, corrosion costs the United States $276 billion,[4] approximately 3.1% of the gross domestic product, and many approaches have been used to understand and model this complex process.[5−7] High-performance stainless steel alloys contain chromium resulting in the formation of a Cr_2O_3 passivating surface layer, which provides corrosion resistance. Even with this layer, such alloys are susceptible to breakdown in acidic, chlorine-containing, aqueous environments,[8,9] the study of which demands simultaneous treatment of surfaces, reactants, and the aqueous dielectric environment. Direct experiments are difficult, and although ab initio calculations have a history of answering many such questions, to date they have not been able to address the effect of the solvent on surface reactions. Alavi et al.,[10] for instance, have studied the adsorption of HCl on single-crystal α-Al_2O_3 (0001) surfaces and calculated adsorption energies as a function of surface coverage within density-functional theory, but all of their results are obtained in a vacuum environment.

Previous studies of Cr_2O_3 have been limited to pure surfaces in a vacuum,[11] an unrealistic environment for the study of corrosion. These studies indicated that the highest occupied and lowest unoccupied molecular orbitals (HOMOs and LUMOs) are localized on the chromium ions, suggesting that the oxygen-terminated surface could provide a stable barrier against acidic chlorinated environments *if* the surface oxygen layer could be prevented from reacting with species in the solution. The work below puts forth evidence to support the novel hypothesis that the dielectric screening effects associated with an aqueous environment actually prevent the formation of bonds with aqueous species such as protons, thereby rendering the oxygen-terminated surface virtually nonreactive.

Models for calculating solvation energies from continuum dielectric theory[12] have been applied to single molecules or activated complexes but not to molecules adsorbed on surfaces, perhaps because such methods are generally applied to molecules. Here, we introduce the first approach to ab initio calculations in a continuum dielectric environment which sits on a firm theoretical foundation. Below, we show that this new approach, which in a simple approximation is related to that recently introduced by Fattebert and Gygi,[13] gives results in good agreement with currently accepted quantum chemical methods and is well-suited to surfaces. Finally, we apply the approach to carry out the first ab initio study of the reactivity of hydrogen and chlorine on an oxygen-terminated Cr_2O_3(0001) surface in contact with a solution.

2. Theoretical Approach: Joint Density-Functional Theory

Because of the large cells required in this study (well over one hundred atoms), the only practicable ab initio approach suited to describe the electrons of the surface and the reactants is the density-functional theory.[11] The size of the surface cell and time scales needed for proper thermodynamic averaging make a direct molecular dynamics treatment of the aqueous environment infeasible, thus raising the question of how to treat the solvent. To do so within a rigorous framework, we introduce here for the first time the concept of a joint density-functional theory (JDFT) between the electrons in the surface and the molecules comprising the solvent. This new theory affords the opportunity to maintain a density-functional treatment of the electrons of the system of interest while giving a rigorous description of the solvent in terms of so-called "classical" density-functional theories,[14] which treat water rigorously in terms of a simple thermodynamically averaged molecular density and a functional to which computationally tractable approximations are known.[15]

A straightforward combination of Mermin's nonzero temperature formulation of density-functional theory[16] with Capitani

* To whom correspondence should be addressed. E-mail: sap23@cornell.edu.
† Cornell University.
‡ Merrimack College.

10.1021/jp044822k CCC: $30.25
Published on Web 07/26/2005

et al.'s extensions of the zero-temperature theory to include nuclear degrees of freedom[17] leads to the following: exact variational principle for the total thermodynamic free energy of an electron−nuclear system in a fixed external electrostatic potential $V(r)$

$$A = \min_{n_t(r),\{N_i(r)\}} \{F[n_t(r),\{N_i(r)\}] + \int d^3r\, V(r)(\sum_i Z_i N_i(r) - n_t(r))\} \quad (1)$$

where $n_t(r)$ is the thermally and quantum mechanically averaged total single-particle density of electrons, $N_i(r)$ is the likewise averaged density of the nuclear species i (of atomic number Z_i), and F is a universal functional. (Here, as throughout this work, we employ atomic units, in which Planck's constant and the mass and charge of the electron all have value unity, $\hbar = m_e = e = 1$.) The universality properties of the functional F may be seen directly from its construction within Levy's constrained search procedure[18]

$$F[n_t(r),\{N_i(r)\}] \equiv \min_{\hat{\rho}\to[n_t(r),\{N_i(r)\}]} \mathrm{Tr}\,(\hat{\rho}\hat{H}_{int} + k_B T\hat{\rho}\ln\hat{\rho}) \quad (2)$$

where $k_B T$ is the thermal energy, $\hat{H}_{int}$ represents all interactions among and the kinetic energy of the electrons and nuclei, and $\hat{\rho}$ is the full quantum-mechanical density matrix for the electron and nuclear degrees of freedom, and the minimization is carried out over only those $\hat{\rho}$ values which lead to the given densities $n_t(r)$ and $\{N_i(r)\}$. From this construction, it is clear that F, like the $\hat{H}_{int}$ value from which it derives, is independent of the external potential $V(r)$ and depends only upon the identities of the nuclear species i (and, implicitly, upon the temperature T), as Capitani et al.[17] found previously for the case of $T = 0$.

To employ the variational principle (eq 1) in the study of a system to be treated explicitly in contact with a solvent environment, we take the nuclear species i to be those comprising the environment (solvent) and the potential $V(r) \equiv \sum_I Z_I/|r - R_I|$ to be that arising from the nuclei of the explicit system (solute), which we take to sit at fixed locations R_I with atomic numbers Z_I. Note that, although we employ a Born−Oppenheimer approximation for the nuclei of the explicit system, at this stage the treatment of the nuclear species of the environment in eq 2 is fully quantum mechanical. Thus, eqs 1 and 2 account for all zero-point motion effects associated with lighter nuclear species in the solvent, such as may be associated with the protons in liquid water or with the helium atoms in superfluid helium when used as a solvent.

Although eqs 1 and 2 give a rigorous continuum treatment of the environment nuclei, the variational principle in eq 1 is ultimately impracticable because it requires explicit treatment of all of the electrons, including those associated with the environment. We thus "integrate out" the electrons associated with the environment by writing $n_t(r) = n(r) + n_e(r)$, where $n_e(r)$ is the electron density associated with the environment and $n(r)$ is the electron density associated with the system in contact with that environment. We then perform the minimization over all allowable $n_e(r)$ values and finally perform the minimization over all allowable $n(r)$ values. For this purpose, we define the sets of allowable $n_t(r)$, $n_e(r)$, and $n(r)$ to be all N-representable functions satisfying the criteria of Gilbert[19] and integrating to the appropriate number of electrons for the respective system. Because all thus defined $n_t(r)$ values can be constructed as the sum of some allowable $n_e(r)$ and some allowable $n(r)$ values and because all such allowable $n_e(r)$ and $n(r)$ values sum to an allowable $n_t(r)$, this procedure is guaranteed to recover the final free energy in eq 1. Thus, we have

$$A = \min_{n(r),\{N_i(r)\}} \{G[n(r),\{N_i(r)\},\{Z_I,R_I\}] - d^3r\, V(r)n(r)\} \quad (3)$$

where $V(r)$ is the electrostatic potential of the nuclei of the explicit system defined above and where

$$G[n(r),\{N_i(r)\},\{Z_I,R_I\}] \equiv \min_{n_e(r)} \left\{ F[n(r) + n_e(r),\{N_i(r)\}] + \sum_I \int d^3r \frac{Z_I(\sum_i Z_i N_i(r) - n_e(r))}{|r - R_I|} \right\} \quad (4)$$

is universal in the sense that its functional form, like F from which it derives, depends only on the nature of the solvent (and, implicitly, the temperature).

Equation 3 gives the exact free energy and exact configuration of the solvent $\{N_i(r)\}$. However, care must be taken in the interpretation of the $n(r)$ which yields the minimum value. The indistinguishablity of electrons implies that there can be no fundamentally meaningful assignment of electrons as belonging either to the environment or to the system, and thus no exact formulation can give a unique result for $n(r)$ without some additional prescription. Indeed, for the exact $\{N_i(r)\}$ value and any $n(r)$ which integrates to the correct number of electrons and is everywhere less than the exact solution $n_t(r)$ and for which $n_e(r) = n_t(r) - n(r)$ is allowable in the above sense, the minimization in eq 4 will find $n_e(r) = n_t(r) - n(r)$ and thus, ultimately, produce the exact value for A. There is thus a large set of $n(r)$ values which yield the minimum value in eq 3, and the variational principle embodied in eqs 3 and 4 satisfies the fundamental condition of not enforcing any particular, arbitrary decomposition of the total electron density into solvent and environment contributions.

In practice, however, we expect approximations to eq 4 to break the above degeneracy and to pick out a unique solution. The standard pseudopotential method, which replaces the effects of the nuclei and (relatively) inert core electrons of a solid or molecule with an effective or "pseudo" potential,[20] is in fact an example of an approximation which tracks only a portion of the total electron density and provides results approaching chemical accuracy while suffering no pathologies related to the underlying degeneracy of an apportionment of electrons between two subsystems. Vaidehi et al.,[21] and later Kim, Park, and co-workers,[22,23] have generalized the pseudopotential approach to closed-shell molecular environments such as water. They replace the effects of the nuclei and electrons of a collection of molecules on the electrons of an external system (solute) with an effective, "molecular pseudopotential" $V_{\{R_i\}}(r)$, which depends explicitly on the locations of the molecular nuclei $\{R_i\}$. Using a total Hamiltonian which includes (a) the interaction between the electrons and nuclei of the external system, (b) the usual internal electron-gas components, but of the external system alone, (c) the interaction of the external electrons with the molecular pseudopotential, and (d) a model potential function $U(\{R_i\},\{R_I\})$ describing the interactions among the environment molecules and the interaction between those molecules and the nuclei of the solute, Vaidehi et al. found the solvation energy of Li^+ to within 0.6 kcal/mol and Kim, Park, and co-workers found results for total energies with an accuracy acceptable for the study of the problem of an excess electron solvated in water.

The existence and reliability of such molecular pseudopotential Hamiltonians implies the existence of reliable approximations to eq 4 which pick out a unique solution for $n(r)$. Formulating the exact thermodynamics of such Hamiltonians with the same approach that leads to eq 1 gives directly the principle in eq 3, but now with

$$G[n(r),\{N_i(r)\},\{Z_I,R_I\}] \equiv \min_{\hat{\rho}\rightarrow[n(r),\{N_i(r)\}]} \mathrm{Tr}(\hat{\rho}\hat{H}_{\{R_i\},\{R_I\}} + k_B T_\rho \ln \hat{\rho}) \quad (5)$$

where $n(r)$ represents the electron density associated with the solute alone and $\hat{H}_{\{R_i\},\{R_I\}}$ represents components (b−d) of the total Hamiltonian described above. Because the electrons have been already apportioned between the solute and the solvent during the construction of $\hat{H}_{\{R_i\},\{R_I\}}$, the functional G in eq 5 represents an example of an approximation to eq 4 which is both reliable and free of any potentially pathological issues associated with degenerate solutions for $n(r)$.

With the functional dependence of G established in eq 3, we next separate out known components and leave an unknown part to be approximated

$$G[n(r),\{N_i(r)\},\{Z_I,R_I\}] \equiv A_{\mathrm{KS}}[n(r),\{Z_I,R_I\}] + A_{\mathrm{lq}}[\{N_i(r)\}] + U[n(r),\{N_i(r)\},\{Z_I,R_I\}] \quad (6)$$

where $A_{\mathrm{KS}}[n(r),\{Z_I,R_I\}]$ is the standard universal Kohn−Sham electron-density functional of the explicit system when in isolation, $A_{\mathrm{lq}}[\{N_i(r)\}]$ is the "classical" density functional for the liquid solvent environment when in isolation, and $U[n(r),\{N_i(r)\},\{Z_I,R_I\}]$, defined formally and exactly as the difference between the exact functional and the sum of the two former functionals, is a new functional describing the coupling between the systems. The new functional $U[n(r),N(r),\{Z_I,R_I\}]$ has the same universal properties as the functional G from which it derives.

While the availability of classical density-functional approximations to A_{lq}[15] makes eq 6 an attractive starting point for future work, in this first work, we make the further simplification of performing the minimization over $\{N_i(r)\}$, resulting in the variational principle

$$A = \min_{n(r)} (A_{\mathrm{KS}}[n(r),\{Z_I,R_I\}] - \int \mathrm{d}^3r\, V(r)n(r) + W[n(r),\{Z_I,R_I\}])$$

where

$$W[n(r),\{Z_I,R_I\}] \equiv \min_{\{N_i(r)\}} (A_{\mathrm{lq}}[\{N_i(r)\}] + U[n(r),\{N_i(r)\},\{Z_I,R_I\}]) \quad (7)$$

is universal in the sense that its functional form depends solely upon the identity of the environment (and, implicitly, the temperature). Note that, in principle, the theory at this stage is exact. Below we outline the approximations which we introduce because the exact forms of the functionals $A_{\mathrm{KS}}[n(r),\{Z_I,R_I\}]$ and $W[n(r),\{Z_I,R_I\}]$ are unknown.

3. Computational Details

For treatment of the electrons in the chromium oxide surface through the functional $A_{\mathrm{KS}}[n(r),\{Z_I,R_I\}]$, we apply the standard local spin-density approximation (LSDA).[24] The calculations themselves employ the total-energy, plane-wave, density-functional, pseudopotential approach[20] with potentials of the Kleinman−Bylander form[25] with p and d nonlocal corrections at a cutoff point of 40 hartrees. Supercells with periodic boundary conditions in all three dimensions represent the surfaces of isolated oxygen-terminated (0001)-oriented slabs of Cr_2O_3 of a thickness of 13 Å separated by 7.8 Å of either vacuum or solvent. The inplane boundary conditions suffice to describe 2×2 reconstructions and consist of 4 times the unit from Cline et al.[11] so as to allow sufficient isolation of solvent volumes excluded by chlorine adsorbed on the surface. The supercell contains a total of 40 chromium and 72 oxygen atoms with chlorine or hydrogen added to the two surfaces in inversion-symmetric pairs, one on each side of the slab. Finally, we use a single k-point to sample the Brillioun zone of the surface slab. Cline et al.[11] also established that this choice of functional, pseudopotential, plane-wave cutoff, sampling density in the Brillioun zone and supercell gives a good description of the bulk and surface of Cr_2O_3. As in the aforementioned work, we employ the analytically continued functional approach[20,26] to minimize the Kohn−Sham energy with respect to the electronic degrees of freedom. Below, we relax all ionic configurations until the total energy is within 0.027 eV of the minimum and the maximum force in any direction is less than 0.3 eV/Å.

For the environment functional $W[n(r),\{Z_I,R_I\}]$ in eq 7, we take the interaction of the electron and nuclear charges of the system under study with a dielectric environment in which the dielectric constant is local in space and has a value dependent only upon the electron density at each point, $\epsilon(r) \equiv \epsilon(n(r))$. Taking in this way the dielectric interaction to be the most significant and modeling it with a local approximation to the dielectric constant is standard practice in semiempirical quantum-chemical continuum dielectric models[27] but does not take direct account of molecular-scale effects such as changes in the dielectric response near the surface due to effects like hydrogen bonding with the surface. Writing the dielectric constant as a function of the explicit electron density allows the electronic structure to determine the boundary between the solvent environment and the explicit system, an approach which Fattebert and Gygi have shown to reproduce well and results from the quantum-chemistry literature.[13] For a more detailed calculation in the future, one could improve upon our results by including a small number of water molecules explicitly at the surface of the system or by employing the more detailed variational principle of eq 6 with approximate functionals which account for nonlocal dielectric effects as well as surface tension associated with the solid−liquid interface.

In practice, we implement the above model for W by computing the total free energy of the system in contact with the environment as the stationary point with respect to both the electrons and the mean electrostatic field $\phi(r)$ of the functional

$$A = A_{\mathrm{TXC}}[n_\uparrow(r),n_\downarrow(r)] + \Delta V_{\mathrm{ps}}[n_\uparrow(r),n_\downarrow(r)] - \int \mathrm{d}^3r \left\{ \phi(r)(n_{\mathrm{tot}}(r) - \sum_I Z_I \delta^{(3)}(r-R_I)) - \frac{\epsilon(n(r))}{8\pi}\left|\nabla\phi(r)\right|^2 \right\} \quad (8)$$

where $n_\uparrow(r)$, $n_\downarrow(r)$, and $n_{\mathrm{tot}}(r)$, respectively, are the up, down, and total electron densities, $A_{\mathrm{TXC}}[n_\uparrow(r),n_\downarrow(r)]$ is the Kohn−Sham single-particle kinetic plus exchange correlation energy within the local spin-density approximation, ΔV_{ps} is the difference in the total pseudopotential energy from that expected from pure Coulombic interactions with point ions of valence charges Z_I at locations R_I, and $\delta^{(3)}(r)$ is the three-dimensional Dirac-δ function. Note that, although we do work directly with the Kohn−Sham orbitals, for brevity we have written the above in

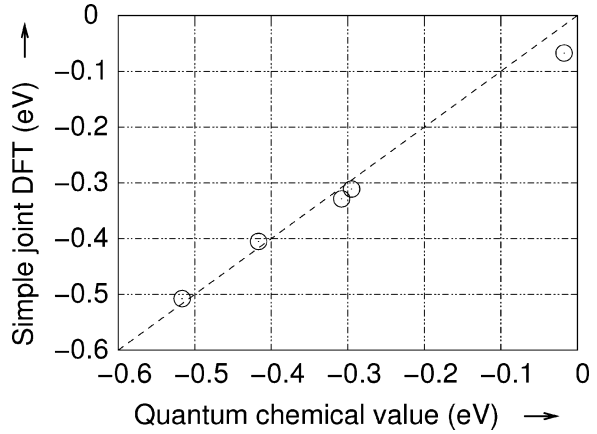

Figure 1. Comparison of the predictions of a simple joint-density-functional theory (vertical axis) with established quantum chemical values (horizontal axis) for the electrostatic contribution to the solvation energy of acetamide, acetic acid, methanol, ethanol, and methane (from left to right) from Marten et al.[28]

terms of the electron densities. We also note that at this level of approximation our JDFT takes the same form as the approach of Fattebert and Gygi,[13] which introduced the form as a computational device without formal justification. Finally, we were able to implement this approach with relatively modest changes to our group's preexisting density-functional software. The primary change was to combine the calculation of the Hartree field (potential from the electrons) and the ionic potential (local part of the ionic pseudopotential) into a single solution of Poisson's equation in the presence of the dielectric function $\epsilon(n(r))$.

For the local dielectric function $\epsilon(n(r))$, we choose a specific form which varies smoothly from the dielectric constant of the bulk solvent ϵ_b when the electron density $n(r)$ is less than a critical value n_c indicative of the interior of the solvent to the dielectric constant of a vacuum $\epsilon = 1$ when $n(r) > n_c$. Specifically, we take

$$\epsilon(n) = 1 + \frac{\epsilon_b - 1}{2}\,\mathrm{erfc}\left(\frac{\ln(n/n_c)}{\sqrt{2}\sigma}\right) \tag{9}$$

where the parameter σ, to which the results are not very sensitive, controls the width of the transition from bulk to vacuum behavior. (Note that Fattebert and Gygi[13] have introduced and justified a very similar form to model $\epsilon(n)$.) To determine the parameters σ and n_c for this simple model, we fit computed electrostatic solvation energies in aqueous solution ($\epsilon_b = 80$) to the accepted values from the quantum-chemical literature for methane, ethanol, methanol, acetic acid, and acetamide.[28] Figure 1 summarizes the quality of this comparison for our final choice of fit parameters, $\sigma = 0.6$ and $n_c = 4.73 \times 10^{-3}$ Å^{-3}.

4. Results and Discussion

4.1. Pristine Surface. Cline et al.[11] review in detail the structure of bulk Cr_2O_3 and the relaxation of its pristine (0001) oxygen-terminated surface. Figure 2 shows the relaxed structure of our supercell surface slab. The bulk structure consists of alternating planar layers of oxygen atoms separated by bilayers of chromium. As Cline et al.[11] also find, the primary relaxation associated with forming the surface is for the oxygen-terminated surface layers to move inward toward the bulk crystal with slight inplane displacements.

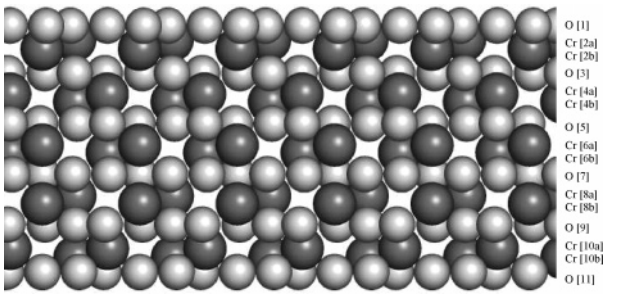

Figure 2. Relaxed structure of a pristine surface slab, side view ([0001] direction runs vertically up the page): oxygen (light gray spheres) and chromium (dark gray spheres). The labeling of atomic layers follows Cline et al.[11]

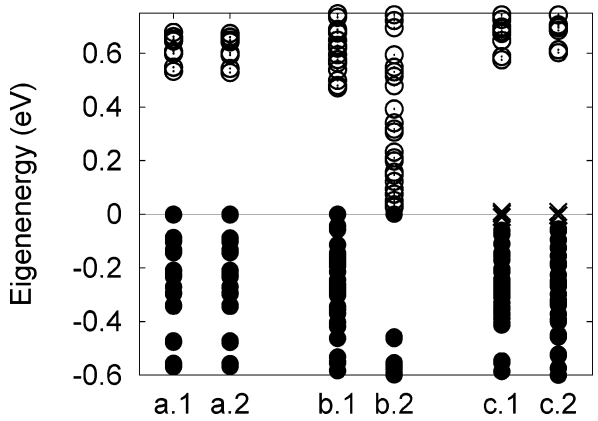

Figure 3. Near-gap energy levels for (a) pristine, (b) hydrogenated, and (c) chlorinated system in (1) a vacuum and (2) dielectric: filled levels (solid circles), empty levels (open circles), and partially filled levels (crosses).

Figure 3a.1 shows the filled and empty energy levels from our supercell calculation of the (0001) oxygen-terminated surface of Cr_2O_3 in a vacuum environment. Following standard practice, we chose the zero of energy to be the Fermi level, the energy below which states are fully occupied and above which they are empty. The states at the zero line in the figure are thus the HOMOs and the first states above the line are the LUMOs. The figure shows the levels of the pristine surface to be fully filled up to a gap of about 0.5 eV separating the HOMOs and LUMOs.

To provide a more global view, Figure 4 presents the density of states, the number of levels from Figure 3a.1 per unit energy as a function of energy, computed using a Gaussian broadening of width $\sigma = 0.41$ eV. To underscore the distinction between occupied and unoccupied states, the figure gives a separate curve for each. Finally, as a guide to the identification of the bands, the figure also contains markers for the LSDA atomic eigenvalues of oxygen and chromium, which have been shifted uniformly upward by 4.4 eV to approximately counteract the shifting of the Fermi level of the supercell states to zero energy. Although there may be no a priori reason to expect neutral atomic eigenvalues to be relevant for this ionic system, we find below that detailed inspection of the corresponding local densities indicates that the features in the density of states correspond precisely in spin orientation, localization, and orbital character to those of the nearby atomic states indicated in the figure.

Three features in the supercell density of states play important roles in the chemistry of this surface. First, the highest occupied *oxygen* orbitals appear as the shoulder (from ca. −4 to ca. −2 eV) of the oxygen 2p band, which consists of "minority" spin

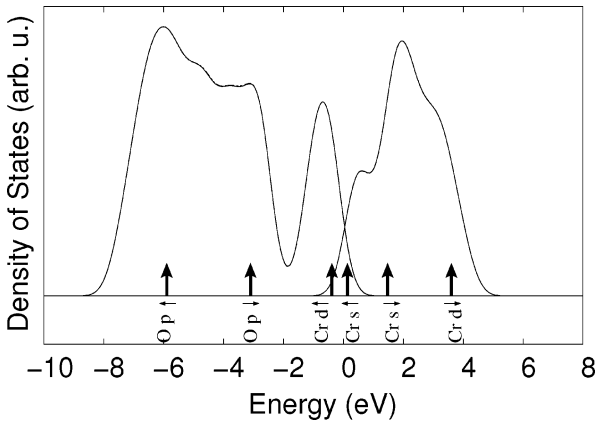

Figure 4. Total density of states of pristine supercell slab in a vacuum (solid curve) and in solution (virtually indistinguishable dashed curve): occupied states (curve on left), unoccupied states (curve on right), and LSDA atomic eigenvalues (vertical arrows) labeled according to alignment (↑) or antialignment (↓) with direction of net atomic spin.

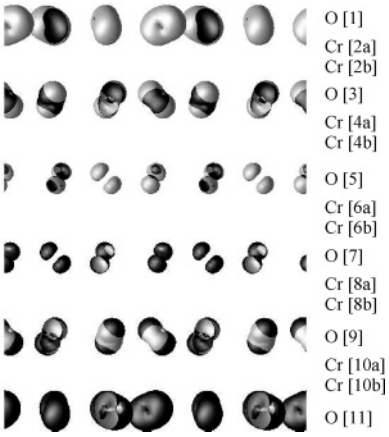

Figure 5. Contour level (0.68 $e^-/Å^3$) of the sum of probability densities from the highest energy shoulder of the oxygen 2p band, side view ([0001] direction runs vertically up the page): up spin (black surface) and down spin (white surface). Locations of atomic layers are indicated as in Figure 2.

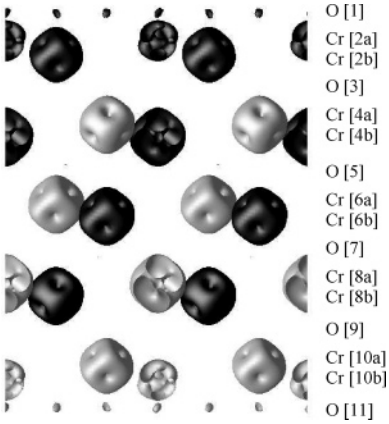

Figure 6. Contour level (0.68 $e^-/Å^3$) of the sum of probability densities from the chromium sd↑ band, side view ([0001] direction runs vertically up the page): up spin (black surface) and down spin (white surface). Atomic layers indicated as in Figure 2.

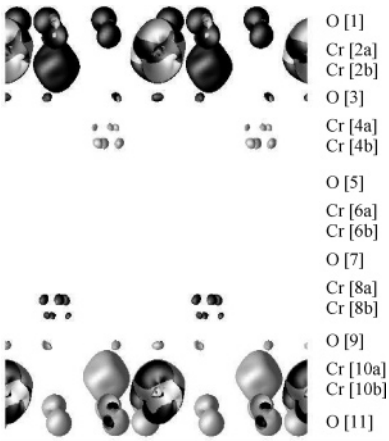

Figure 7. Contour level (0.68 $e^-/Å^3$) of the sum of probability densities from the lowest energy shoulder of the chromium sd↓ spin band, side view ([0001] direction runs vertically up the page): up spin (black surface) and down spin (white surface). Atomic layers indicated as in Figure 2.

electrons, electrons with spin opposite to the net atomic spin. Figure 5a presents the sum of the probabilities associated with states in this range and clearly indicates this shoulder to be a surface oxygen band. (The contour level in this and all subsequent electron density maps is set at the same value of 0.68 $e^-/Å^3$, chosen so as to make evident the localization and orbital character of the corresponding states.) The localization of different spin types to either surface corresponds to the fact that the oxygen atoms on each surface have an opposite net spin direction. Next, the HOMOs overall appear as an sd-hybrid chromium band (from ca. −2 to ∼0 eV) consisting of electrons of "majority" spin and spin aligned with the net atomic spin. Figure 6 shows these states to be *bulk* chromium states, with atoms alternating in majority spin direction corresponding to the antiferromagnetic nature of the bulk material. Finally, the LUMOs of the system appear as the low energy majority spin shoulder (from ∼0 H to ∼1 eV) of an empty chromium band. Figure 7 shows this shoulder to consist of surface states of primarily chromium character protected under the outer oxygen layer. This character of the HOMOs and LUMOs suggests that any oxygen missing from the outer surface would expose a reactive chromium layer underneath.

Upon repeating the pristine surface calculation in the presence of a dielectric environment, we find virtually no change. There is no change in Figure 2, and although some very small changes are evident in going from Figure 3a.1 to Figure 3a.2, the global picture of the density of states in Figure 4 is visually indistinguishable for a vacuum (solid curve) and a dielectric (dashed curve). Finally, inspection of density maps corresponding to Figures 5−7 again shows no noticeable changes.

4.2. Interaction with Hydrogen. Anticipating bonding with oxygen, we initially placed a hydrogen atom in a vacuum directly on top of one of the surface oxygen atoms, all of which are equivalent by symmetry. Figure 8a shows that, upon relaxation, the hydrogen atom cants away from the surface perpendicular while appearing to form a bond with the underlying oxygen atom: the final relaxed O−H distance is 0.95 Å, quite close to the experimental O−H separation in H_2O (0.96 Å). Figure 9 shows that the canting of the hydrogen atom is in the same direction as one would expect for the 2p orbital of the associated oxygen atom given its inplane displacement. Finally, Figure 10a, which shows the total electron density associated with the chemisorbed H, confirms the presence of the bond as a small protrusion in the density near the hydrogen atom.

Figure 3b.1 shows the filled and empty energy levels of the hydrogenated surface in a vacuum environment. As with the pristine surface (Figure 3a), the energy levels are fully filled up to a HOMO−LUMO gap, consistent with the observed bonding. To better resolve the bond associated with the chemisorbed hydrogen, Figure 11 presents the *local* density of

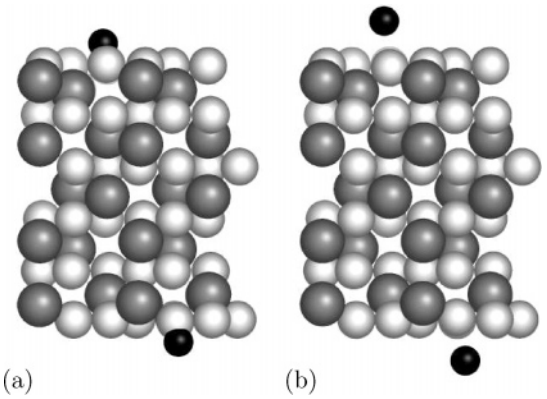

Figure 8. Relaxed structure of surface slab with adsorbed hydrogen in (a) a vacuum and (b) dielectric: oxygen (light gray spheres), chromium (dark gray spheres), and hydrogen (black spheres). Same view as Figure 2 but showing atoms from a single supercell.

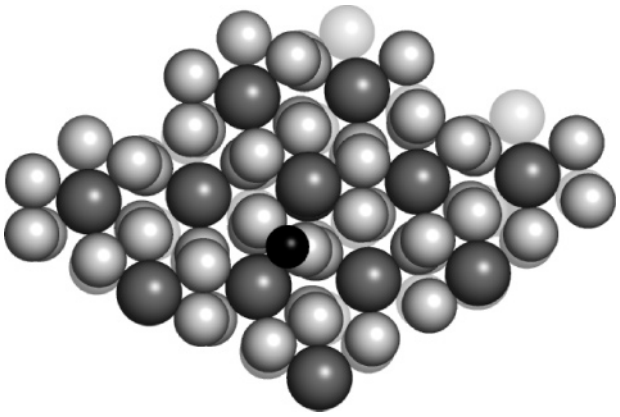

Figure 9. Relaxed structure of a single supercell with adsorbed hydrogen in a vacuum, top view ([0001] direction normal to page): oxygen (light gray spheres), chromium (dark gray spheres), and hydrogen (black sphere).

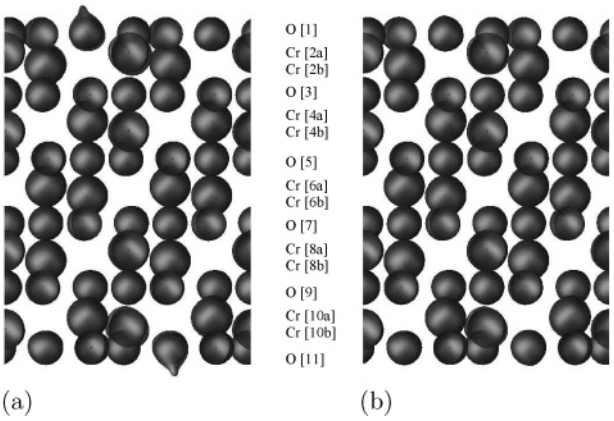

Figure 10. Contour level (0.68 $e^-/Å^3$) of total electron density for hydrogen atom adsorbed on oxygen-terminated (0001) surface in (a) a vacuum and (b) a dielectric, side view ([0001] direction runs vertically up the page). Atomic layers indicated as in Figure 2.

states in the vicinity of the hydrogen atom, which we compute in the same way as the total density of states of Figure 4 but by now weighing each level with the probability of an electron in the level being within 0.69 Å of the proton. The local density of states shows that the hydrogen atom interacts mostly with the surface oxygen 2p band. A plot of the total density associated with this surface band, Figure 12a, confirms that it contains most of the density protrusion associated with the O−H bond. Finally, Figure 13a shows that the HOMO of the hydrogenated

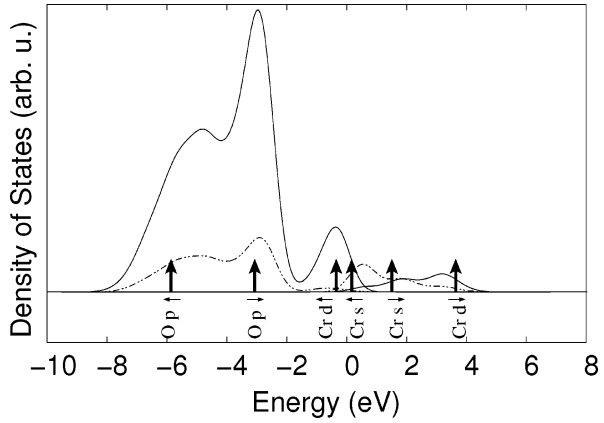

Figure 11. Local density of states within 0.69 Å of the proton for hydrogen interacting with oxygen-terminated (0001) surface in a vacuum (solid curve) and solution (dashed curve). Same conventions as Figure 4.

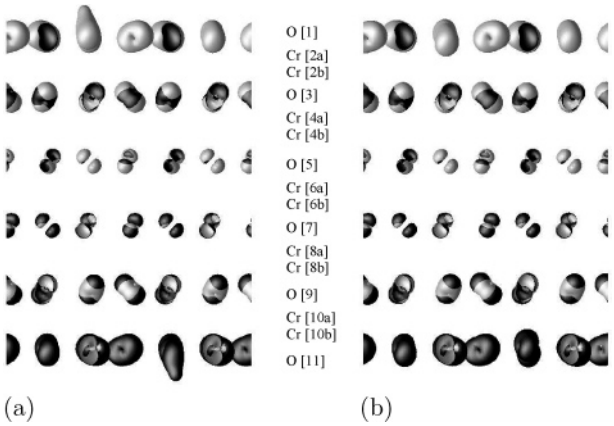

Figure 12. Contour level (0.68 $e^-/Å^3$) of the sum of probability densities associated with the oxygen 2p surface band in (a) a vacuum and (b) a dielectric: up spin (black surface) and down spin (white surface). Atomic layers indicated as in Figure 2.

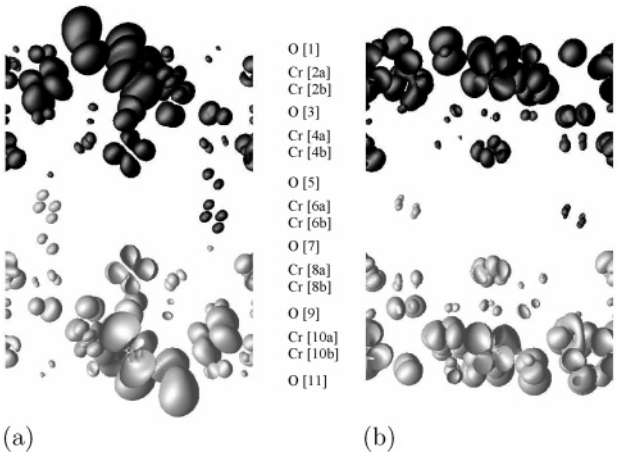

Figure 13. Contour level (0.68 $e^-/Å^3$) of the HOMO of hydrogen interacting with the oxygen-terminated (0001) surface in (a) a vacuum and (b) a dielectric, side view ([0001] direction runs vertically up the page): up spin (black surface) and down spin (white surface). Atomic layers indicated as in Figure 2.

surface, while maintaining significant bulk chromium character, indeed localizes near the hydrogen atom.

To determine the final atomic configuration in the presence of a solvent, we began with the positions from Figure 8a and relaxed the atomic coordinates within the approximate joint density functional of eqs 8 and 9 until the maximum force on

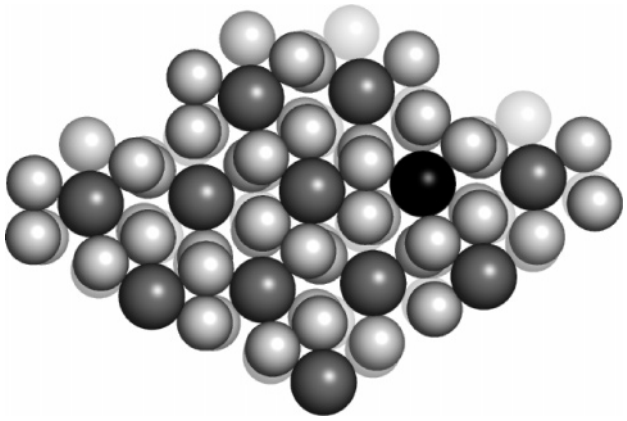

Figure 14. Relaxed structure of surface interacting with chlorine in a vacuum: oxygen (light gray spheres), chromium (dark gray spheres), and chlorine (black sphere): top view ([0001] direction perpendicular to page).

any atom was less than 0.3 eV/Å. Figure 8b, which displays the resulting configuration, shows that the presence of the dielectric has a dramatic effect on the hydrogen. The nearest oxygen−hydrogen distance increased to 2.3 Å, clearly breaking the O−H bond and returning the hydrogen atom to the solution. Consistent with this picture, the largest residual force remains on the hydrogen atom in the direction tending to push it yet further from the surface. Lack of any indication of the presence of the hydrogen atom in the resulting total charge density, Figure 10b, indicates that the atom enters the solution as an ion.

Figure 3b.2 shows that upon the removal of the proton from the surface, the excess electron from the O−H bond appears simply as a donated conduction electron just above the energy gap. Consistent with this donation, the dashed curve in Figure 11 shows a dramatic reduction in the local density of states near the proton, and the HOMO in Figure 13b now shows more of the surface chromium character of the original LUMO band from Figure 7.

4.3. Interaction with Chlorine. Anticipating the possibilities of ionic bonding for chlorine, we initially placed (in the 1×1 surface supercell) a chlorine atom in a vacuum directly above each of the two distinct types of Cr^{3+} site from the outermost chromium bilayer and found the site above the innermost of the two component layers to be favored by 0.4 eV. Figure 14 shows a top ([0001]) view of the relaxed configuration for this site when computed within the 4×4 supercell. We find relatively little relaxation from the clean surface structure (movement of all surface atoms is less than 0.01 Å) with the chlorine ion settling upon relaxation to a position with a chlorine−oxygen separation of 2.6 Å, only 20% smaller than the sum of the nominal ionic radii, 3.1 Å. Figure 15a shows a side view of the total electron density for a surface with adsorbed Cl in a vacuum, illustrating the physisorbed nature of the interaction.

Turning to the energy levels, Figure 3c.1 shows the levels near the gap. In this case, three two-thirds filled states (degenerate to within 19 meV, ~220 K) appear just below the top of the gap, indicating the presence of a hole in the Cr band, which we interpret as arising from the chlorine atom absorbing an electron from the chromium oxide to become Cl^-. To explore local effects from the adsorbed chlorine, Figure 16 presents the local density of states, weighing each state with the probability of an electron being within 1.6 Å of the chlorine nucleus. In contrast to the local density of states of the hydrogen calculation, the appearance of the oxygen band is significantly reduced and there is much stronger mixing with the bulk chromium states.

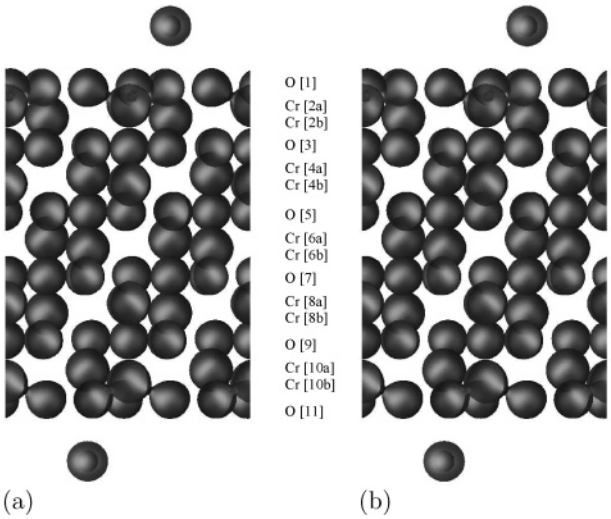

Figure 15. Contour level (0.68 $e^-/Å^3$) of total electron density for chlorine atom adsorbed on oxygen-terminated (0001) surface in (a) a vacuum and (b) a dielectric, side view ([0001] direction runs vertically up the page). Atomic layers indicated as in Figure 2.

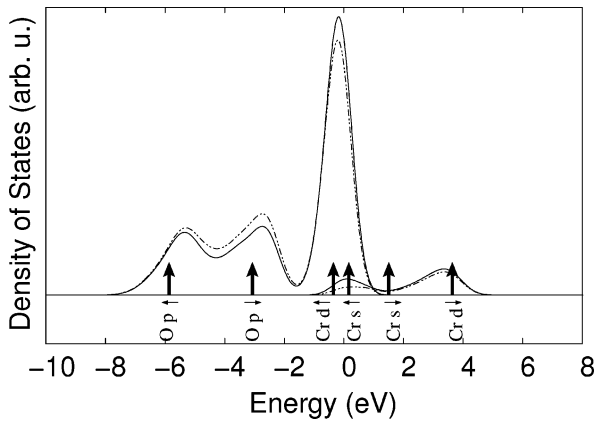

Figure 16. Local density of states within 1.6 Å of the chlorine nucleus for chlorine interacting with the oxygen-terminated (0001) surface in a vacuum (solid curve) and solution (dashed curve). Same conventions as Figure 4.

This mixing corresponds to an alignment of the barely bound Cl^- states with the bulk HOMO chromium band as the chlorine ion draws electrons from the bulk chromium band, which is serving as a reservoir of electrons. Finally, Figure 17a shows the sum of the electron probabilities in the partially filled states at the Fermi level, which are thus both the HOMOs and the LUMOs. Interpreted as the sum of states lacking exactly one electron from full occupancy, the figure shows the spatial distribution of the hole which the formation of the Cl^- injects into the chromium oxide slab. As one would expect, this (positive) hole tends to localize to the vicinity of the Cl^- ions.

Upon relaxation of the physisorbed chlorine surface in the presence of the solvent, we find there to be very little relaxation (no more than 0.01 Å for any atom), little difference in the total charge density (Figure 15b), no change in the presence of partially filled states at the Fermi level (Figure 3c.2), and very little difference in the local density of states (Figure 16) or the spatial distribution of the hole injected into surface, Figure 17b.

4.4. Conclusions. Above, we introduce the novel approach of using a joint density-functional theory to treat an ab initio electronic structure calculation in the presence of a liquid solvent such as water. The resulting approach is the first ab initio approach for the treatment of the interaction of complex surfaces

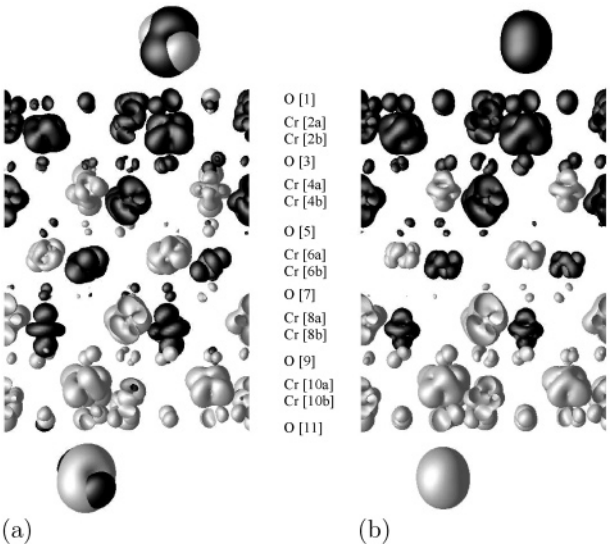

Figure 17. Contour level (0.68 $e^-/Å^3$) of HOMOs and LUMOs (equivalent in this case) of chlorine interaction with oxygen-terminated (0001) surface in (a) a vacuum and (b) a dielectric, side view ([0001] directions runs vertically up the page). Atomic layers indicated as in Figure 2.

with chemical species in the presence of a molecular environment to treat that environment rigorously in terms of a continuum.

Through this approach, we find the mode of interaction of the oxygen-terminated Cr_2O_3 (0001) surface with hydrogen to be covalent bonding while that with chlorine to be ionic bonding. The presence of a dielectric solvent has very little effect on the pristine surface or on its interaction with chlorine, while it has a dramatic affect on the interaction with hydrogen. In a vacuum, hydrogen readily forms an O−H bond with the outermost layer of atoms of the surface. In the presence of water, the strong screening associated with dielectric effects in the vicinity of the proton (ultimately via hydrogen bonding interactions) so weakens the attractive potential of the proton that the covalent bond is broken, the electron is released into the surface, and the proton solvates.

In contrast, the interaction with chlorine in a vacuum is already ionic, with a neutral chlorine atom having sufficient electronegativity to draw an electron from the bulk of the crystal and thus ionize to Cl^- while injecting a hole into the bulk. The presence of a dielectric solvent tends to screen the excess charge on the chlorine ion, thereby only further stabilizing this form of interaction with the surface so that there is little change in this case when going from vacuum to a dielectric environment. It thus appears that the primary reason the solvent has a much greater effect on the interaction with hydrogen than with chlorine is that a dielectric environment generally favors the formation of ions and the surface interaction with chlorine is already ionic whereas the interaction with hydrogen in a vacuum is covalent.

We believe that there would be little effect on these conclusions were the calculations to be performed with ions rather than atoms. Doing so would involve principally removing a single electron from the calculation for each hydrogen atom or adding an electron for each chlorine atom. For the chlorine cases, this would simply remove the relatively delocalized hole from the bulk chromium band and thus likely have little effect on the final results. For the interaction with hydrogen, the removal of an electron from our calculation as performed currently would, in the dielectric case, likely simply remove the relatively delocalized donated electron or, in the vacuum case, likely simply introduce a relatively delocalized hole into the chromium band. In either of these cases for hydrogen, we again would expect little change in the results of our calculations. To make a definitive statement for the precise behavior of a proton on the surface, future calculations should include a more detailed variational principle of eq 6 and at least a few water molecules so as to allow for the Grotthus mechanism (proton diffusion via bond switching events in the water environment). However, allowing the Grotthus mechanism would seem only to make departure of the proton into the solution more likely. Thus, although we cannot draw a definitive conclusion at this point, we feel that with protons, as we have found with hydrogen atoms, there will be little disruption of the chemical integrity of the surface.

Overall, a novel picture emerges to explain how the oxygen-terminated surface of Cr_2O_3 is particularly protective in a hydrochloric acid solution. The outer oxygen layer provides a natural barrier to interaction with chlorine but might be expected to interact strongly with protons. However, through dielectric screening effects, it is the aqueous environment itself which eliminates the outer oxygen layer's natural tendency to interact with hydrogen.

These first calculations of surface chemistry in the presence of a solvent make clear the need for additional work to complete the picture of the passivating effects of chromium oxide. We would next like to study the interaction of chlorine and hydrogen with a *chromium*-terminated surface, whose HOMOs would then be exposed on the surface rather than protected under the outer oxygen layer. We also would like to explore pit corrosion by calculating the interaction of the aforementioned species with a step in the passivating oxygen layer. Finally, we would like to contrast the interactions of chlorine in such systems to the interactions of fluorine and bromine in order to better understand the corrosive success of chlorine relative to these other species.

Acknowledgment. This work was funded by NSF Grant No. CHE-0113670. A.A.R. would like to thank Jefferson W. Tester and Ronald M. Latanision for planting the seed of this project during her 1994−1995 sabbatical at MIT.

References and Notes

(1) Radeke, M. R.; Carter, E. A. *Annu. Rev. Phys. Chem.* **1997**, *48* (1), 243−270.
(2) Greeley, J.; Norskov, J. K.; Mavrikakis, M. *Annu. Rev. Phys. Chem.* **2002**, *53*, 319−348.
(3) Gross, A. *Surf. Sci.* **2002**, *500* (1−3), 347−67.
(4) DeGaspari, J. *Mech. Eng.* **2003**, *125* (9), 30.
(5) Ryan, M. P.; Williams, D. E.; Chater, R. J.; Hutton, B. M.; McPhail, D. S. *Nature* **2002**, *415* (6873), 770−774.
(6) Stampfl, C.; Ganduglia-Pirovano, M. V.; Reuter, K.; Scheffler, M. *Surf. Sci.* **2002**, *500* (1−3), 368−394.
(7) Erlebacher, J.; Aziz, M.; Karma, A.; Dimitrov, N.; Sieradzki, K. *Nature* **2001**, *410* (6827), 450−3.
(8) Jones, D. A. *Principles and Prevention of Corrosion*; Prentice Hall: Upper Saddle River, NJ, 1996.
(9) Latanision, R.; Mitton, D.; Zhang, S.; Cline, J.; Caputy, N.; Arias, T. In *Fourth International Symposium on Supercritical Fluids*; Sendai, Japan, 1997; Vol. C, pp 865−868.
(10) Alavi, S.; Sorescu, D. C.; Thompson, D. L. *J. Phys. Chem. B* **2003**, *107* (1), 186−195.
(11) Cline, J. A.; Rigos, A. A.; Arias, T. A. *J. Phys. Chem. B* **2000**, *104* (26), 6195−6201.
(12) Tannor, D.; Marten, B.; Murphy, R.; Friesner, R.; Sitkoff, D.; Nicholls, A.; Ringnalda, M.; Goddard, W.; Honig, B. *J. Am. Chem. Soc.* **1994**, *116* (26), 11875−.
(13) Fattebert, J.-L.; Gygi, F. *J. Comput. Chem.* **2002**, *23* (6), 662−666.
(14) Curtin, W.; Ashcroft, N. *Phys. Rev. A* **1985**, *32* (5), 2909−19.
(15) Sun, S. *Phys. Rev. E* **2001**, *64* (2), 021512−1.
(16) Mermin, N. *Phys. Rev.* **1965**, *137* (5A), A1441−A1443.

(17) Capitani, J.; Nalewajski, R.; Parr, R. *J. Chem. Phys.* **1982**, *76* (1), 568−73.
(18) Levy, M. *Proc. Natl. Acad. Sci. U. S. A.* **1979**, *76* (12), 6062−6065.
(19) Gilbert, T. *Phys. Rev. B* **1975**, *12* (6), 2111−20.
(20) Payne, M.; Teter, M.; Allan, D.; Arias, T.; Joannopoulos, J. *Rev. Mod. Phys.* **1992**, *64* (4), 1045−97.
(21) Vaidehi, N.; Wesolowski, T.; Warshel, A. *J. Chem. Phys.* **1992**, *97* (6), 4264−71.
(22) Kim, K.; Park, I.; Lee, S.; Cho, K.; Lee, J. L.; Kim, J.; Joannopoulos, J. *Phys. Rev. Lett.* **1996**, *76* (6), 956−9.
(23) Park, I.; Cho, K.; Lee, S.; Kim, K.; Joannopoulos, J. *Comput. Mater. Sci.* **2001**, *21* (3), 291−300.
(24) Perdew, J.; Wang, Y. *Phys. Rev. B* **1992**, *45* (23), 13244−9.
(25) Kleinman, L.; Bylander, D. *Phys. Rev. Lett.* **1982**, *48* (20), 1425−8.
(26) Arias, T.; Payne, M.; Joannopoulos, J. *Phys. Rev. Lett.* **1992**, *69* (7), 1077−80.
(27) Tomasi, J.; Persico, M. *Chem. Rev.* **1994**, *94* (7), 2027−94.
(28) Marten, B.; Kim, K.; Cortis, C.; Friesner, R. A.; Murphy, R. B.; Ringnalda, M. N.; Sitkoff, D.; Honig, B. *J. Phys. Chem.* **1996**, *100* (28), 11775−11788.